Journal of Fundamental and Applied Sciences

Research Article

ISSN 1112-9867

Available online at http://www.jfas.info

BIOMETRIC VERIFICATION SYSTEM BASED ON HAND GEOMETRY

K. Harrar

LIST Laboratory, University M'Hamed Bougara of Boumerdes, Algeria

Received: 22 September 2020 / Accepted: 15 January 2021 / Published online: 01 May 2021

ABSTRACT

Biometric systems are widely used in medium and low security applications. Verification systems based on the geometry of the hand utilize some geometrical characteristics of the hand including measurements of fingers, shape of the palm, etc. In this work, we have developed an unconstrained and contact-based hand geometry verification system, using a combination of length and width of fingers. New measurements at different points of fingers were introduced in this paper to improve the performance of the recognition of persons. A total of 135 hand images were enrolled in this study. The Euclidean distance was used as a similarity function for different values of threshold. The proposed method was compared to state-of-the-art approaches. The results obtained reveal the high performance of the proposed approach and outperformed the existing methods with an accuracy of Acc = 98.67%.

Keywords: Biometric; hand geometry; length and width; verification system

Author Correspondence, e-mail: khaled.harrar@univ-boumerdes.dz

doi: http://dx.doi.org/10.43 14/jfas.v13i2.11

1. INTRODUCTION

Biometrics is a technique of measurments of human characteristics utilized to identify or authentify persons in groups of individuals. It is based on "what we are" and "how we behave" [1]. Hand geometry uses the fingers and palm shape, including palm area, widths,

and lengths of fingers in several places, etc. These hand characteristics are suitable in verification systems (personal authentification). Moreover, the combination of these features allows to achieve good results. This technique is widely accepted and the verification includes simple data processing. The charcateristics listed make the hand geometry a good candidate to research and develop new identification and verification approches [2-4].

The human hand incorporates various anatomical features used in biometric applications, but is not enough for a complete individual identification. In fact, the geometry of the hand can change during the time due to illness, body weight, and aging. To overcome this, recent reseach deal with normal persons with no illness, no high changing in weight, and adults (avoiding young persons which hand can grew). It is actually based on the fact that every person has a differently formed hand which will not drastically change in the future [3,5,6].

Several works have been done on the geometry of the hand systems. Burgues et al. [7], found that the least discriminative features in a hand geometry system are related to the palm geometry and thumb shape for 50 users, and they have concluded that the widths and the lengths of four fingers are the most discriminative features.

Gross et al. [8] presented a technique based on Active Appearance Models (AAM) to track the hand inside the capture device and to extract geometry features for identification. The authors stated that the AAM algorithm executed in less time than in real-time. They used a small dataset of the hand images (18 persons). The similarity measure used was the Euclidian distance, and the accuracy of their system yielded 90%. Goh et al. [9] proposed a biometric contactless system based on the geometry of the hand using infrared and color imagery. An acquisition system was developed to capture both infrared and color hand images. Five features including hand geometry, palmar knuckle, palm (print, and vein), and finger are used for recognition. Experiments were carried out to testify the performance of the system and yielded a mean error of EER = 2.2%. Chawkat et al. [10] developed an automatic recognition system with a neural network model. The authors used morphological features (segmentation) including the geometry of all fingers and palm, extracted from a typical database. The experiments were performed on 500 images (50 persons, 10 images for each one). The performance of their system achieved an accuracy of 96.41%.

Although these methods provide acceptable results, they lack in computational accuracy and efficiency. For this reason, there is a scope to enhance the hand-based system.

The objective of this work is to develop a hand geometry verification system for recognizing people, which in the medium and low-security applications can replace traditional methods (password, badge, etc.), that can be stolen, lost, or forgotten. This system is cheaper and user-friendly in comparison with constrained and contactless based of the geometry of the hand systems. This work aims to compare the lengths and the widths of fingers. We focus on which is the most discriminative geometrical features between the lengths and the widths of four (04) fingers (without the thumb). In the first step, we have conducted six experiments corresponding to lengths and widths of fingers separately. In the second stage, we have combined lengths and widths features of fingers and introduced new features related to fingers' lengths and widths at several points of the hand, to enhance the recognition rate and accuracy. Moreover, a comparative study involving the proposed approach and some methods existing in the literature was conducted. The main contributions of this work are:

- Creation of a new database of hands images
- Development of a biometric system combining lengths and widths of fingers
- Introduction of new lengths and widths measurements of fingers
- Improvements results comparing to the state-of-the-art methods

The remainder of this article is strutured as follows: Section 2 presents the methodology and acquisition system. Section 3 provides results and discussion, and section 4 concludes this work.

2. METHODOLOGY

In this paper, a personal verification system (one to one) by using the hand geometry features is proposed. The block diagram is shown in Fig. 1.

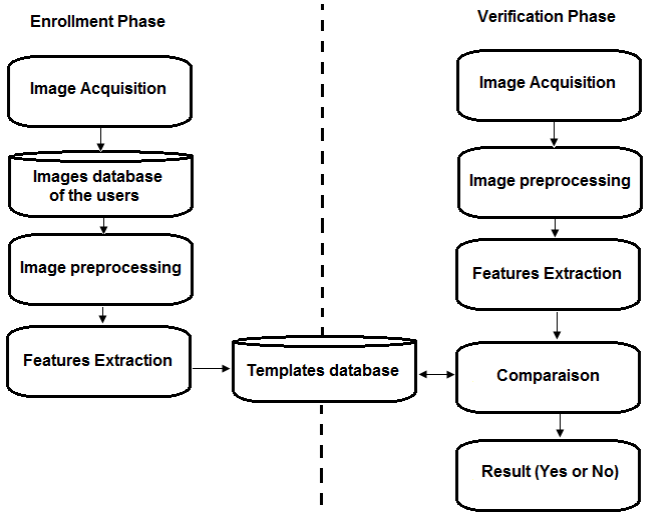

Fig.1. Flowchart of hand geometry verification system

The system is divided into two parts, the enrollment, and the verification steps. Both steps use the same pre-processing techniques to obtain hand-geometry features. In the enrollment step, the features extracted from the users' hands are stored in a database. In the verification setp, the Euclidean distance metric is used to measure the similarity existing between an applicant person and a known hand image in the database, to decide if the system accept or not the claimant.

2.1. Enrollment

In this stage, several images of the hand are taken from each user by a normal document scanner. The images are saved in a database called "images database of the users". The system takes the training set of a user's images from this database, preprocesses them, and extracts from each image a vector containing the necessary features. Finally, the system estimates the mean vector of these training sets of images, and stores it in a database called "Templates database".

2.1.1. Image acquisition and dataset

In this work, we have created our database containing 135 images. The hand images are obtained from the user group composed of family members and friends, and stored in the database called "Images database of the users". For this purpose, a normal document scanner 'Canon i-SENSYS MF3010' was used. The user can put its hand freely because there are no pegs to set the position of the hand. In our experiments, only the right-hand images of the

users were acquired. The parameters of the scanner were set as follow:

- Digitalization mode: color
- Image resolution output: 637 × 637 pixels

During the acquisition process, the users were requested to stretch their fingers and put their palm straight on the platform of the scanner with slightly different poses. To ensure a good quality of the acquisition some conditions should be taken in consideration:

- The background should be black. This condition ensures that the histogram of the image will be bimodal, and it facilitates the detection of the edge where are the landmark points. For this, a black box was used as a background to cover the user's hand during the acquisition.
- The user's fingers do not touch each other.
- The scanner surface should be clear (by cleaning the traces due to laying hands).

To test the performance of our system, different authentic images of users and impostors were used as follow:

- 12 authentic users (10 images of the right hand by users). The first five images of authentic users were used for the enrollment phase and the last five images for the verification phase.
- 03 impostors (5 images of the right hand per person) were used to test the performance of the system to detect unauthorized persons.

In total 60 images of authentic users were used in the enrollment phase and 60 images of authentic users + 15 images of impostors were used to test the performances. Fig.2 shows sample hand images of the database.

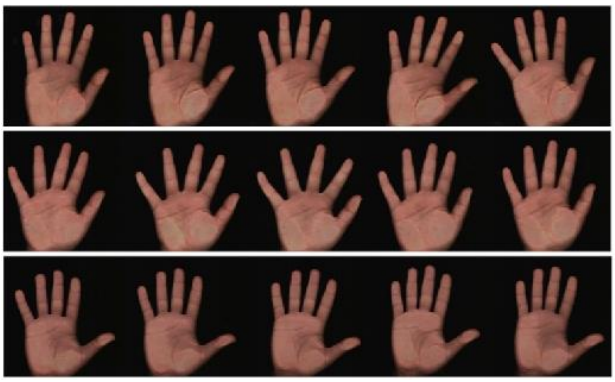

Fig.2. Hand images from the database of users

2.1.2. Image preprocessing

In this section, the preprocessing step was performed including several operations. Fig. 3

illustrates the schema of the preprocessing step.

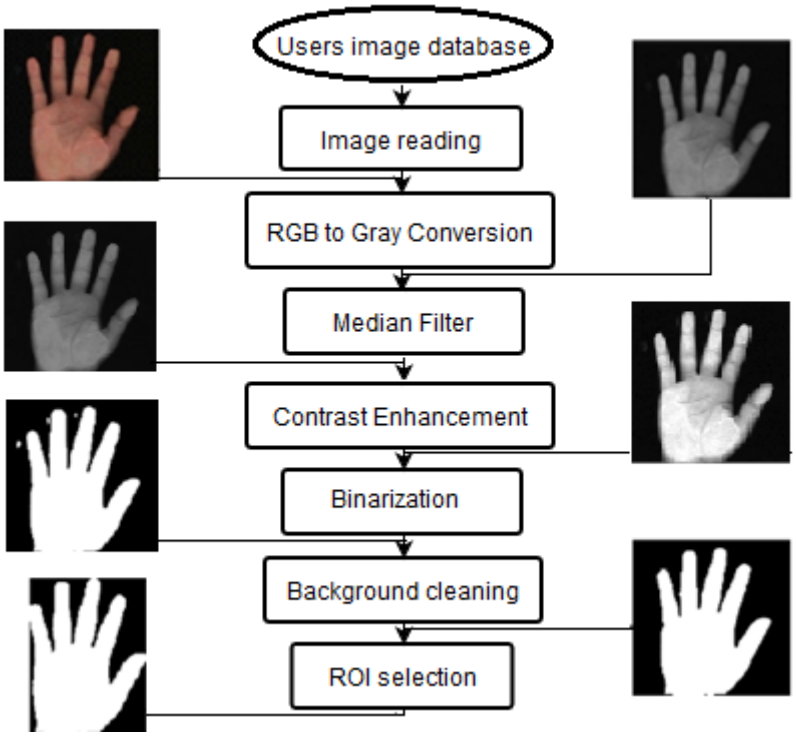

Fig.3. Block diagram of the preprocessing step

- **Conversion from RGB to grayscale**

The image is captured by the scanner in the color map (Fig. 4.a). The system should first convert the image to a gray level (Fig. 4.b).

- **Filtering**

During the process of acquiring images, some undesired pixels appear in the outcome image. These pixels are considered as noise. To remove this noise a median filter was used [11]. It is usually used due to its performance in denoising images, particularly 'salt & pepper' noise. The median filter is nonlinear and consists in replacing the gray level of a pixel by the median value of the gray levels of neighboring pixels, instead of using the average operation (Fig. 4.c).

- **Contrast enhancement**

To improve the quality of the image, enhancement is performed. For this, histogram stretching was used to increase the contrast of an image, which allows making the object of

interest (hand) lighter (Fig. 4.d). Histogram stretching consists of distributing the frequencies of appearance of the pixels on the width of the histogram [12]. It consists to extend the histogram so that the lowest intensity value becomes zero, and highest value becomes the maximum value.

- **Binarization**

Due to the background black color, there is a clear distinction in pixels intensity between the hand and the background. Therefore, the image can be easily converted to a binary image by thresholding (Fig. 4.e). The binarization of an image is performed by replacing all the values' pixels of the image greater than the threshold by 1 (white) and the pixels whose gray levels are below the chosen threshold, by 0 (black). The threshold value is automatically computed using Otsu's method [13].

- **Background cleaning**

During the acquisition stage, and due to the multiple laying of the users' hands, there is an appearance of traces on the surface of the scanner. For this, a cleaning step is necessary to suppress the undesired pixels from the image binary (Fig. 4.f).

- **ROI selection**

To facilitate the use of images and reduce the calculation time, it is suitable to work on an image containing only the hand (Region Of Interest), represented in Fig. 4.g.

(a)

(b)

(c)

(d) (e) (f)

(g)

Fig.4. Preprocessing step used for the hand images. (a) Captured image, (b) grayscale image, (c) filtered image, (d) Enhanced gray image, (e) binary image, (f) background cleaning, (g) ROI selection

2.1.3. Features extraction

The role of this step is to create a vector containing the measurements of discriminative biometric characteristics (the length and the width of fingers at different places) from the binary image created previously. Fig. 5 illustrates the block diagram of the features extraction.

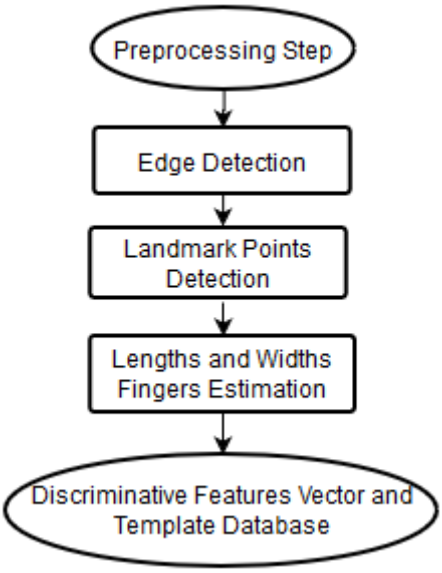

Fig.5. Diagram of the features extraction

- **Edge detection of the hand**

The pixels of the hand contour are obtained from the binary image by using an edge detection method based on Moore-Neighbor tracing method modified by the stopping criteria of Jacob [14]. The process starts by scanning the pixels of the binary image from the bottom-left to the right. When the first white pixel is located, the edge tracing algorithm with eight neighboring pixels is performed to trace the contour of the hand in a clockwise direction. During the edge tracing process, the pixels' coordinates were saved in a matrix (Fig. 6.a).

- **Landmark points**

By plotting the pixels of the hand contour with its raw coordinates as shown in Fig.6.b and Fig. 7.a, we can easily observe that the peak points in the figure correspond to the fingertips points of the hand and by the inversion of the plot we can see the peak points in the inversed plot corresponding to the valley points.

To make measurements, we used additional points (E1 and E2) from the landmark points (Fig. 7.b). The number of contour pixels between P1 and E1 is equal to the number of contour pixels between P1 and V1. Also, the number of contour pixels between P4 and E2 is equal to the number of contour pixels between P4 and V3.

The points M1, M2, M3, and M4 represent the midpoints between (E1, V1) and (V1, V2) and (V2, V3) and (V3, E2) respectively (Fig. 7.c).

The coordinates of a midpoint $M(x,y)$ between two points $p(x_1, y_1)$ and $q(x_2, y_2)$ are given by:

$x = (x_1+x_2)/2 \quad y = (y_1+y_2)/2$

$$M = \left(\frac{x_1+x_2}{2}, \frac{y_1+y_2}{2}\right) \qquad (1)$$

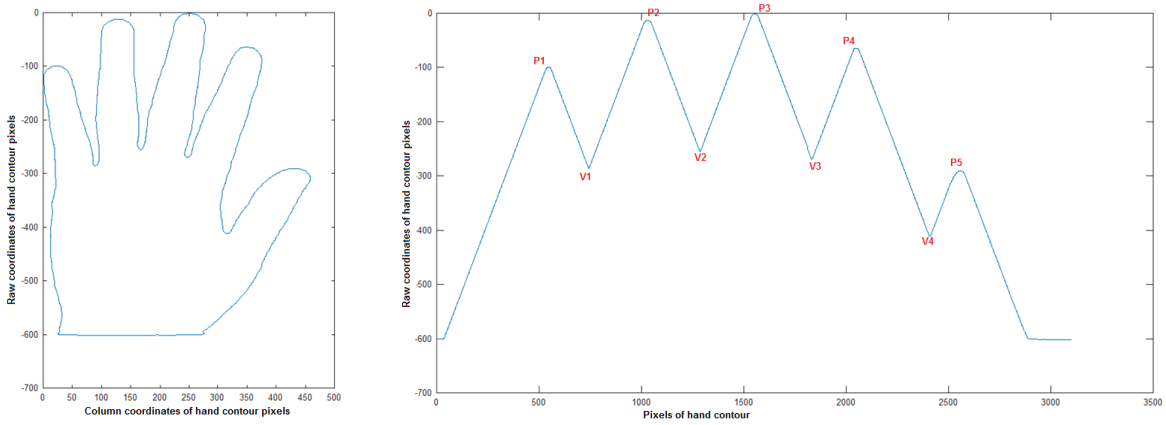

(a) (b)

Fig.6. Edge detection step. (a) Pixels coordinates of hand contour, (b) representation of raw coordinates of hand contour

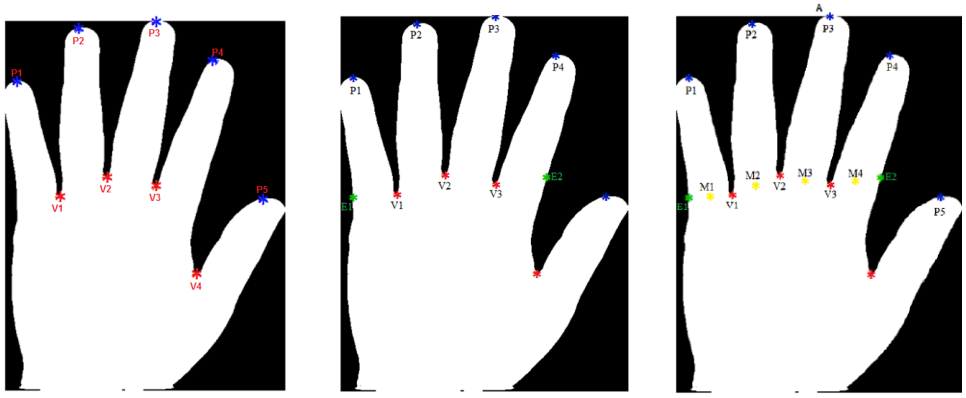

(a) (b) (c)

Fig.7. Representation of the different landmark points. (a) Principal landmark points, (b) added points (E1, E2), (c) midpoints representation

- **Estimation of the lengths and the widths of the fingers**

To calculate the length of the fingers (Fig. 8.a), the added points (E1 and E2) allow precise measurements from the landmark points (Peaks and valleys).

L1 represents the distance separating P1 and M1, and L2 represents the distance separating P2 and M2. L3 represents the distance separating P3 and M3, and L4 represents the distance separating P4 and M4. Eq. 2 was used to compute the Euclidean distance *d* separating two points $p(x_1, y_1)$ and $q(x_2, y_2)$ in a two-dimensional space.

$$d(p,q) = \sqrt{(x_2 - x_1)^2 + (y_2 - y_1)^2} \qquad (2)$$

To calculate the width of the fingers in different places, we have created other points from the landmarks, as shown in Fig.8.b.

For the pinky finger, we divided the portion of the outline between (P1,V1) into three parts. The sum of pixels between (P1, WL2) is then equal to the sum of pixels between (P1, WL1). Same thing between (P1, WL4) and (P1, WL3), and between (P1, WL6) and (P1, WL5).

The procedure is repeated for the other fingers. Note that the annular (ring finger) and middle finger are divided into four portions, and the little finger and forefinger (index) into three portions. Eq.2 is used to estimate the Euclidean distance between two points:

- The measured widths for the little finger are denoted by: WL12 = d(WL1, WL2), WL34 = d(WL3, WL4), WL56 = d(WL5, WL6).
- The measured widths for the annular finger are denoted by: WR12 = d(WR1, WR2), WR34 = d(WR3, WR4), WR56 = d(WR5, WR6), WR78 = d(WR7, WR8).
- The measured widths for the middle finger are denoted by: WM12 = d(WM1, WM2), WM34 = d(WM3, WM4), WM56 = d(WM5, WM6), WM78 = d(WM7, WM8).
- The measured widths for the index finger are denoted by: WI12 = d(WI1, WI2), WI34 = d(WI3, WI4), WI56 = d(WI5, WI6).

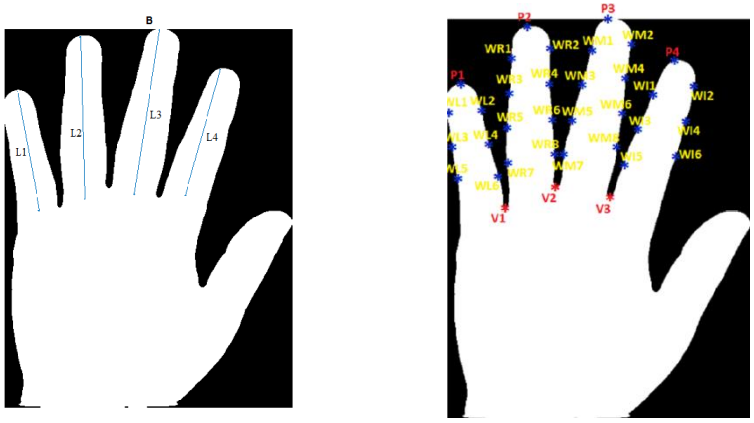

(a) (b)

Fig.8. Lengths and widths of the fingers. (a) Representation of the length, (b) add points for the estimation of the widths

- **Discriminative features vector and template database**

To create a representative vector that will be used for the comparison step, we have used the mean of the vectors of the images chosen for the enrollment step, and stored in the "Template database". This process was repeated for each user.

2.2. Verification

A biometric system is like other authentication systems in that an authorized user has to register oneself to the system before verification or identification can be accomplished [15,16]. The features extracted from the registered person is stored as a template in a database.

The system requests the user to provide an image of his right hand. The system preprocesses the selected image, extracts the biometric characteristics, and creates a single vector of biometric characteristics. Then the system compares this vector with all templates saved in the template database. Finally, the system decides according to a predefined threshold (Th) if it accept or not this user. In this work, the Euclidean distance classifier is used as a parameter to decide whether the user is recognized or not. The Euclidean distance is given by [17]:

$$d = \sqrt{\sum_{i=1}^{L}(t_i - x_i)^2} \qquad (3)$$

Where 'L' is the feature vector dimension, x_i is the i^{th} user's feature vector component, and t_i the i^{th} component of the feature vector saved in the templates database.

Even under the best of conditions, it cannot be expected that characteristics obtained from the user to be identified correspond exactly with the characteristics of its template (of the same individual). For this, the minimum distance Euclidean represents the best similarity [18].

The last step is to decide to accept or not a claimant. For limiting access to registered users (genuine), we used a threshold. It is determined from the different test images (optimal threshold). If the minimum distance is less than the threshold, the system confirms the claimant identity. If the minimum distance is greater than the threshold, the system declares that the claimant is not registered in the database and negates its identity.

2.3. Evaluation of the system

To evaluate the accuracy of a biometric system, the most commonly used metrics are the False Acceptance Rate (FAR) and the False Rejection Rate (FRR). FRR computes the rate of authorized persons rejected by the biometric system and FAR estimates the rate of unauthorized individuals which are accepted in the biometric system. In this study, several metrics are defined [19]:

- False rejected (FR): genuine person classified as false
- False accepted (FA): unauthorized person classified as true
- True rejected (TR): unauthorized person classified as false
- True accepted (TA): genuine person classified as true
- Total persons (TP): number of attempt access
- Equal Error Rate (ERR): point where FAR and FRR have the same value
- Identification Rate (IR): rate of true detections at the optimal threshold
- Accuracy (Acc): describe how accurate a biometric system performs

$$FRR = \frac{FR}{TP} \times 100 \qquad (4)$$

$$FAR = \frac{FA}{TP} \times 100 \qquad (5)$$

$$Acc = 100 - \frac{FAR + FRR}{2} \qquad (6)$$

$$IR_{Th} = \frac{TA}{TP} \times 100 \qquad (7)$$

The Equal Error Rate (ERR), is defined as the compromise between FAR and FRR. It is usually used in the evaluating step the comparaison between biometric systems [20]. The more the EER is near to 0%, the better is the performance of the target system [21].

3. RESULTS AND DISCUSSION

In this section, the results of different experiments are presented. 10 images per person were involved, 5 images of each person were used for the enrollment phase and the other five to test the performance of our biometric system using FRR, FAR, EER, and Acc.

As we stated before, in this work we have introduced new measurements relating to widths and lengths of fingers to improve the performance of the verification system. Fig.9 presents the experiments and the comparison between classical measurements used in the literature and the new measurements used in our work. Concerning the lengths, most of authors used just 1 median length for each finger (Fig.9.a), where we used 3 (1 median and 2 lateral) measurements for each finger (Fig.9.c). Same thing for the widths, the classical measurements used in the literature are just up to 2 widths (Fig.9.d), where we introduced more measurements reaching 8 widths (Fig.9.f).

3.1. Verification system using fingers' lengths

From the landmark points, and by calculating the Euclidean distance between two points, we have done several measurements. The results are reported in Table1.

- **Experiment 1**

The features vector of this experiment is the lengths of the four fingers (except the thumb). Each length is measured from the top of the finger (P1, P2, P3, P4) to the middle points (M1, M2, M3, M4), respectively (Fig.9.a).

The feature vector for this experiment is: F_V1 = [L1, L2, L3, L4].

- **Experiment 2**

The features vector of this experiment is the length of the four fingers (except the thumb) measured at two places for each finger (Fig. 9.b). The features vector for this experiment is: F_V2 = [LL1, LL3, LR1, LR3, LM1, LM3, LI1, LI3].

- **Experiment 3**

The features vector of this experiment is the lengths of the four fingers (except the thumb) measured at three places for each finger (Fig. 9.c). The features vector for this experiment is: F_V3 = [LL1, LL2, LL3, LR1, LR2, LR3, LM1, LM2, LM3, LI1, LI2, LI3].

3.2 Verification system using fingers' widths

- **Experiment 4**

The features vector of this experiment is the widths of the four fingers (except the thumb) measured at different places for each finger (Fig. 9.d). The features vector for this experiment is: F_V4 = [WL34, WR34, WR56, WM34, WM56, WI34].

- **Experiment 5**

The features vector of this experiment is the widths of the four fingers (except the thumb) measured at different places for each finger (Fig. 9.e). The features vector for this experiment is: F_V5 = [WL12, WL34, WL56, WR12, WR34, WR56, WR78, WM12, WM34, WM56, WM78, WI12, WI34, WI56].

- **Experiment 6**

The features vector of this experiment is the widths of the four fingers (except the thumb) measured at different places for each finger (Fig. 9.f). The feature vector for this experiment is: F_V6 = [WL12, WL34, WL56, WL78, WL910, WL1112, WR12, WR34, WR56, WR78, WR910, WR1112, WR1314, WR1516, WM12, WM34, WM56, WM78, WM910, WM1112, WM1314, WM1516, WI12, WI34, WI56, WI78, WI910, WI1112].

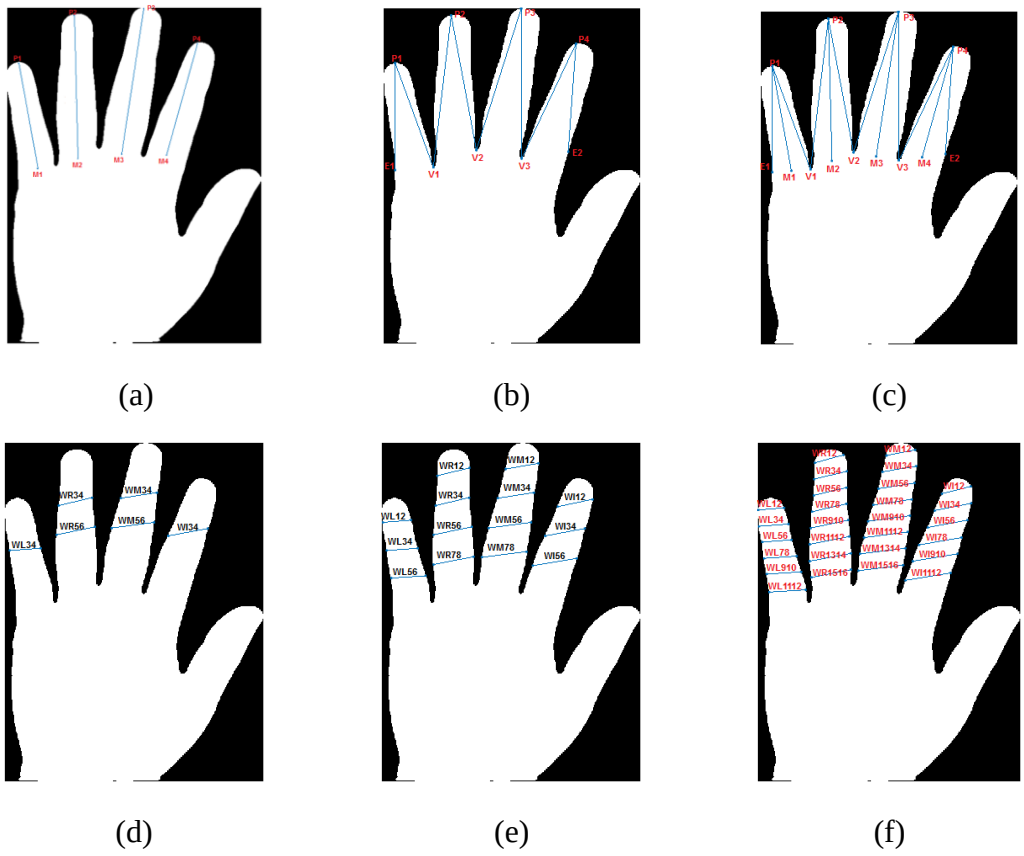

Fig.9. Six experiments relating to the fingers' features. (a) Experiment 1 with four lengths, (b) experiment 2 with eight lengths, (c) experiment 3 with twelve lengths, (d) experiment 4 with six widths, (e) experiment 5 with 14 widths, and (f) experiment 6 with 28 widths

Mainly, the hand geometry systems utilize several geometrical features taken from the hand. Examining the works done in this literature, we have found that the researchers eliminate some geometrical features because they increase the error rate [22 – 24]. However, the effect of some geometrical features (especially the lengths and the widths) is not remarkable in the case of utilizing hand geometry systems with pegs, in which these pegs serve as reference points and keeping the hand in the same position.

In this work, we have developed a verification system based on hand geometry and we have tested it on a database of images taken from 15 users (10 images per user) by the means of a document scanner. Three experiments for only the lengths and three experiments for only the widths. By observing the error rates obtained (Table 1) in these experiments, we found that the performance of this system improved when we have introduced more measurements in

lengths of fingers. The error rate was 3.63% for one length per finger, and decreased to 2.41% for three lengths per finger. Same findings for the widths, by introducing the new measurements the performance increased and the error rate decreased from 5.85% using six widths measurements, to 3.77% using twenty-eight widths measurements. This proves that the new measurements introduced in this study contributes to better classify the persons.

Table 1. Performance of the biometric system for the 6 experiments

Experiment	Features vector	Figure	EER (%)
01	F_V1 = [L1, L2, L3, L4]	9.a	3,63
02	F_V2 = [LL1, LL3, LR1, LR3, LM1, LM3, LI1, LI3]	9.b	3,45
03	F_V3 = [LL1, LL2, LL3, LR1, LR2, LR3, LM1, LM2, LM3, LI1, LI2, LI3]	9.c	2,41
04	F_V4 = [WL34, WR34, WR56, WM34, WM56, WI34]	9.d	5,83
05	F_V5 = [WL12, WL34, WL56, WR12, WR34, WR56, WR78, WM12, WM34, WM56, WM78, WI12, WI34, WI56]	9.e	4,27
06	F_V6 = [WL12, WL34, WL56, WL78, WL910, WL1112, WR12, WR34, WR56, WR78, WR910, WR1112, WR1314, WR1516, WM12, WM34, WM56, WM78, WM910, WM1112, WM1314, WM1516, WI12, WI34, WI56, WI78, WI910, WI1112];	9.f	3,77

3.3. Combining lengths and widths

In this work, we have performed two other experiments regarding the widths and the lengths. We have combined the lengths and the widths of users' hands. Our hand geometry verification system uses both lengths and widths of fingers of the hand to classify the users. Two groups are used:

Group 1: The number of widths measured in this group is 14 widths (3 widths for the pinky (little) finger, 4 widths for the ring finger, 4 widths for the middle finger, and 3 widths for the index finger). Four lengths were also added (L1, L2, L3, L4). The vector characteristics of the group 1 contains 18 distances: Vector_group1 = [L1, L2, L3, L4, WL12, WL34, WL56, WR12, WR34, WR56, WR78, WM12, WM34, WM56, WM78, WI12, WI34, WI56].

Group 2: In this group, we have optimized the number of measured widths. The total number of widths is 6 widths (1 width for the little finger, 2 widths for the ring finger, 2 widths for the middle finger, and 1 width for the index finger). Four lengths were also added (L1, L2, L3, and L4). Moreover, we have introduced new features (3 measurements) corresponding to ratios between lengths of fingers (L3/L1, L2/L4, and length average (L1+L2+L3+L4)/4). The vector characteristics of the group 2 contains 13 distances: Vecteur_groupe2 = [L1, L2, L3, L4, L3/L1, L2/L4, (L1+L2+L3+L4)/4, WL34, WR34, WR56, WM34, WM56, WI34].

Table 2. Performance of the system at different threshold values for the biometric characteristics of group 1.

# Test	Th	FRR (%)	FAR (%)	Acc (%)
01	22	0	100	50
02	21	0	80,33	59,835
03	20	0	75,66	62,17
04	19	0	66,33	66,835
05	18	0	56,66	71,67
06	17	0	23,33	88,335
07	16	0	15,66	92,17
08	15	0,33	9,66	95,005
09	14	1	5,66	96,67
10	13	1,33	1,33	98,67
11	12	8	1,33	95,335
12	11	15	1	92
13	10	20,33	0,66	89,505
14	09	33	0	83,5
15	08	40,66	0	79,67
16	07	56,66	0	71,67
17	06	66,33	0	66,835
18	05	73,66	0	63,17
19	04	78,66	0	60,67
20	03	82,33	0	58,835
21	02	100	0	50

3.3.1. Experiments relating to group 1

In this section, we present the results obtained from group 1 using 18 features. We have tested several values of the threshold to evaluate the performance of our biometric system. The results are reported in Table 2.

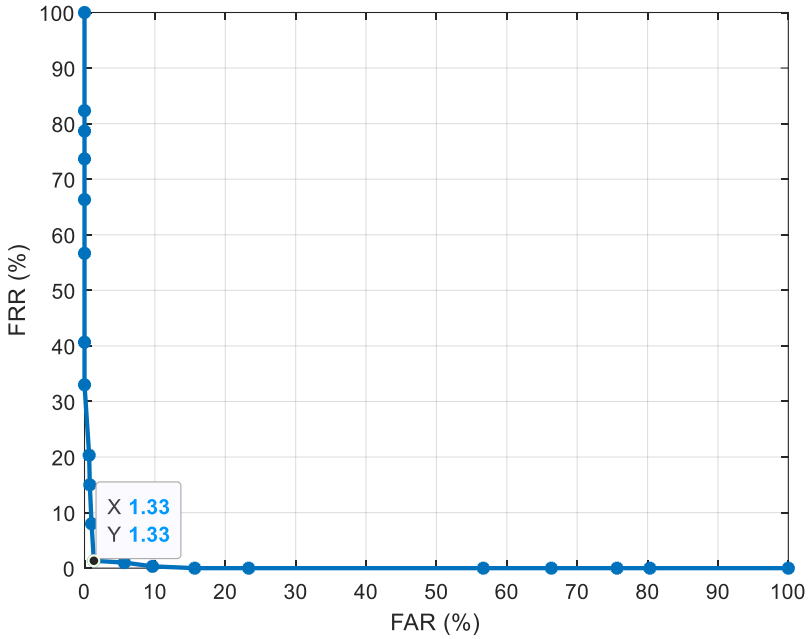

Fig.10. ROC curve for group 1

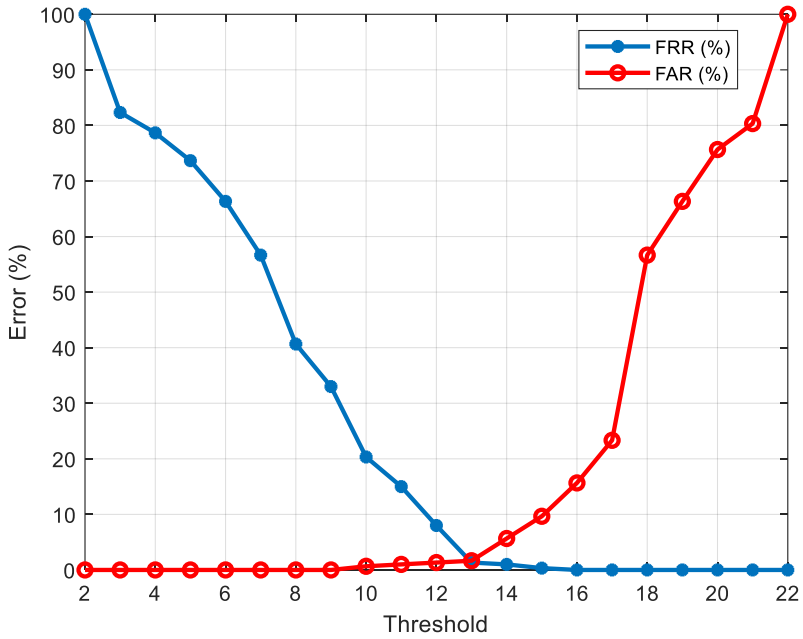

Fig.11. Influence of the threshold in group 1

Figure 10 illustrates the ROC curve [25] representing the rate of false acceptance against the rate of false rejection. The EER was estimated from this figure where FRR = FAR, EER = 1.33%. Regarding the threshold, we have obtained an optimized value of Th = 13 (Fig.11). We can estimate the identification rate at this threshold. We have obtained 55 genuine users which are correctly identified among 60 images of users utilized in the test stage with IR = 91.66%. According to the accuracy, the system achieved a high performance with Acc = 98.67% (Table 2) demonstrating the high performance of our system.

Table 3. Performance of the system at different threshold values for the biometric characteristics of group 2.

# Test	Th	FRR (%)	FAR (%)	Acc (%)
01	20	0	100	50
02	19	0	90,33	54,835
03	18	0	81	59,5
04	17	0	74,33	62,835
05	16	0,66	66,33	66,505
06	15	1	40	79,5
07	14	1,33	33,33	82,67
08	13	1,66	26,66	85,84
09	12	2	15,33	91,335
10	11	2,33	2,33	97,67
11	10	9,66	1	94,67
12	09	25	0,5	87,25
13	08	35,33	0	82,335
14	07	50	0	75
15	06	63,33	0	68,335
16	05	80	0	60
17	04	90	0	55
18	03	98,33	0	50,835
19	02	100	0	50

3.3.2. Experiments relating to group 2

In this section, we descibe the results obtained from group 2 using 13 features. We have tested several values of the threshold to assess the performance of the proposed biometric system.

The results are reported in Table 3.

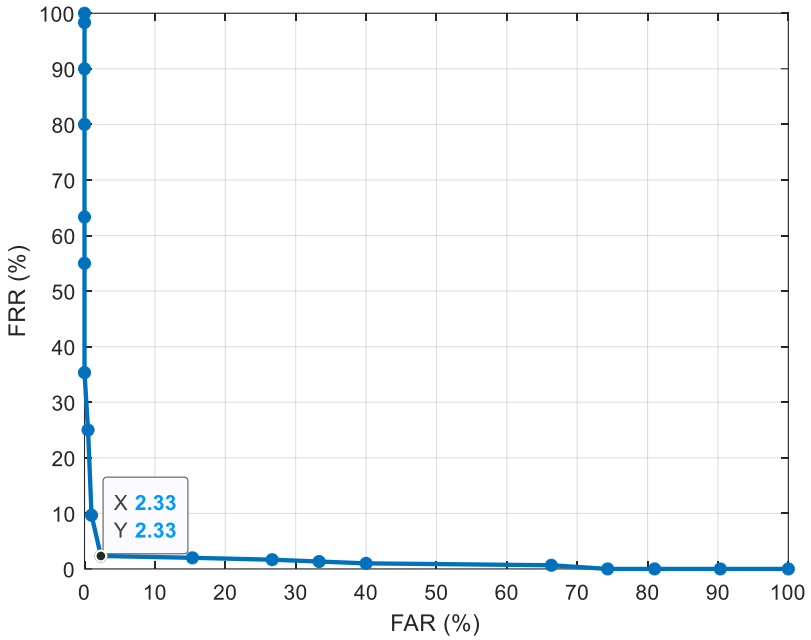

Fig.12. ROC curve for group 2

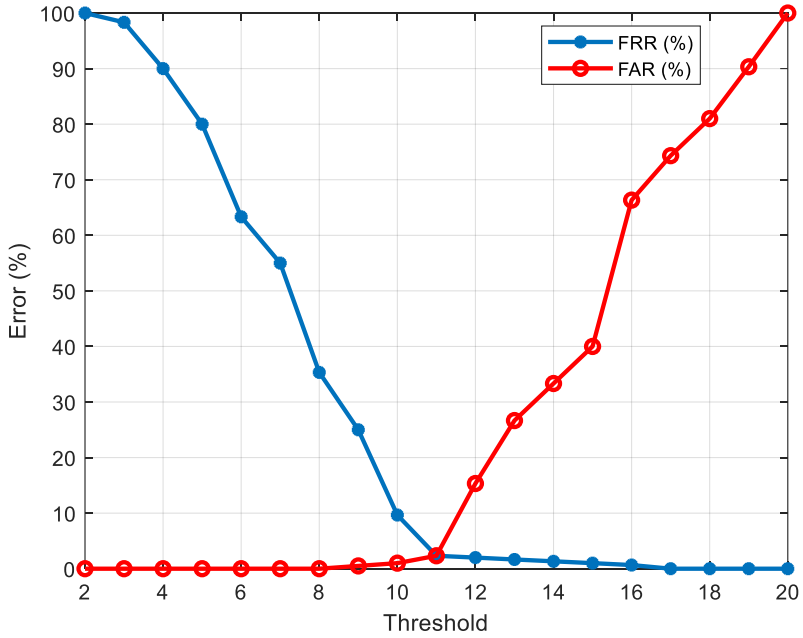

Fig.13. Influence of the threshold in group 2

Figure 12 illustrates the ROC curve plotting the rate of false acceptance versus the rate of false rejection. Figure 13 illustrates the influence of the threshold on the identification of the persons. The EER was estimated from this figure with EER = 2.33%. Regarding the threshold,

we have obtained an optimized value of Th = 11 (Fig.13). We can estimate the identification rate at this threshold. We have obtained 54 genuine users which are correctly identified among 60 images of users utilized in the test stage with IR = 90%. According to the accuracy, the system achieved high performance with Acc = 97.67% (Table 3).

Examining the experiments, we can notice that the lengths of the fingers are more discriminative than their widths. This is because of the finger pressure applied by users during the acquisition stage.

3.4. Comparative study with the state-of-the-art

This section presents state-of-the-art methods used in the literature. The aim is to compare our approach to these methods. Table 4 shows several works done by the authors. Number of persons, features, similarity measure, and performance are reported in the Table. To provide a coherent study, the comparison was done taking in consideration the number of persons enrolled in the methods. For this, we have reported studies using small databases like ours. Studies using huge databases are not reported, because the number of samples influences the performance of the results. As we can see the proposed methods outperforms other methods with the lowest rate of error (EER = 1.33%) this is due to the new measurements introduced to our verification system.

The shape of the finger is not regular [26]. The size of the finger’s bone changes between landmark points. For this, it is important to take many measures in different places to guarantee a good recognition. This is the pupose of our work. The difference between our study and most of the existing studies in the literature is that we use many measures (up to 41 features with 28 widths and 12 lengths for 4 fingers) compared to what other authors use (Table 4).

Table 4. Comparative study of the state-of-the-art methods

Year	Population	Image/ Person	Number/type of templates	Features (Number)	Measure	Performance
Proposed	15	10	1 (average feature vector)	New Finger lengths and widths for four fingers (41)	Euclidian	EER = 1.33%
2000 [27]	20	10	1 (average feature vector)	Finger lengths, widths, ratios thickness, deviation (25)	Hamming, GMM	EER = 5 %
2002 [28]	22	12	2 (average feature vectors)	Finger lengths, widths (13)	GMM probability ratio of hit points	EER = 6.6 %
2008 [29]	40	10	4 (SVM training)	Finger widths for three fingers (40)	SVM	EER = 3.4%
2005 [30]	22	10	2 (MLP and KNN training)	Finger lengths, widths, Hand perimeter and surface (21)	MLP and KNN scores	EER = 6.36

3.5. Application

This section presents an example of the application of the proposed method on images. Figure

14 shows the recognition of a user person belonging to the template database. As we can see a message box appeared stating the true recognition of the person. On the other hand, we have tested an imposter person. For this, we have introduced his hand to the system and tried to look if the system rejects it. Figure 15 illustrates this example, and a message box appeared to state that the imposter was an unauthorized person. These examples demonstrate the performance of our system in recognizing persons.

All the programs developed in this work have been implemented using Matlab 2016 running under Windows 10 on a computer with CPU Intel(R) Core(TM) i7-3632QM @2.20GHz with 8 GB of memory.

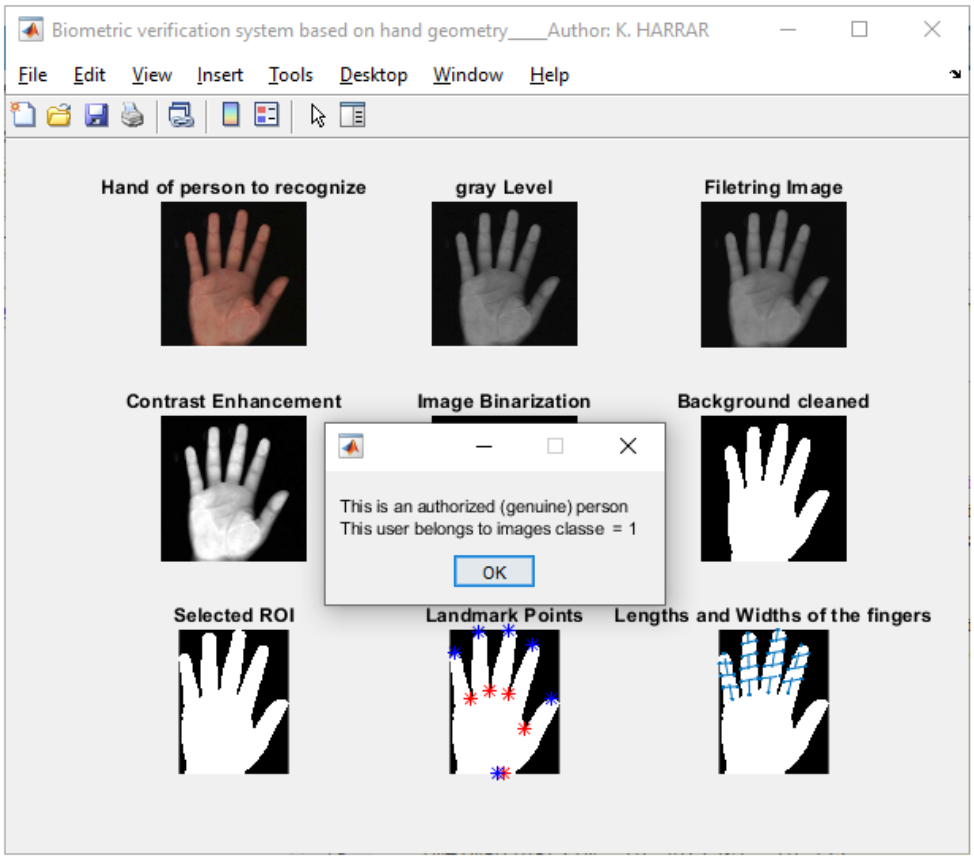

Fig.14. Example of recognizing a genuine user

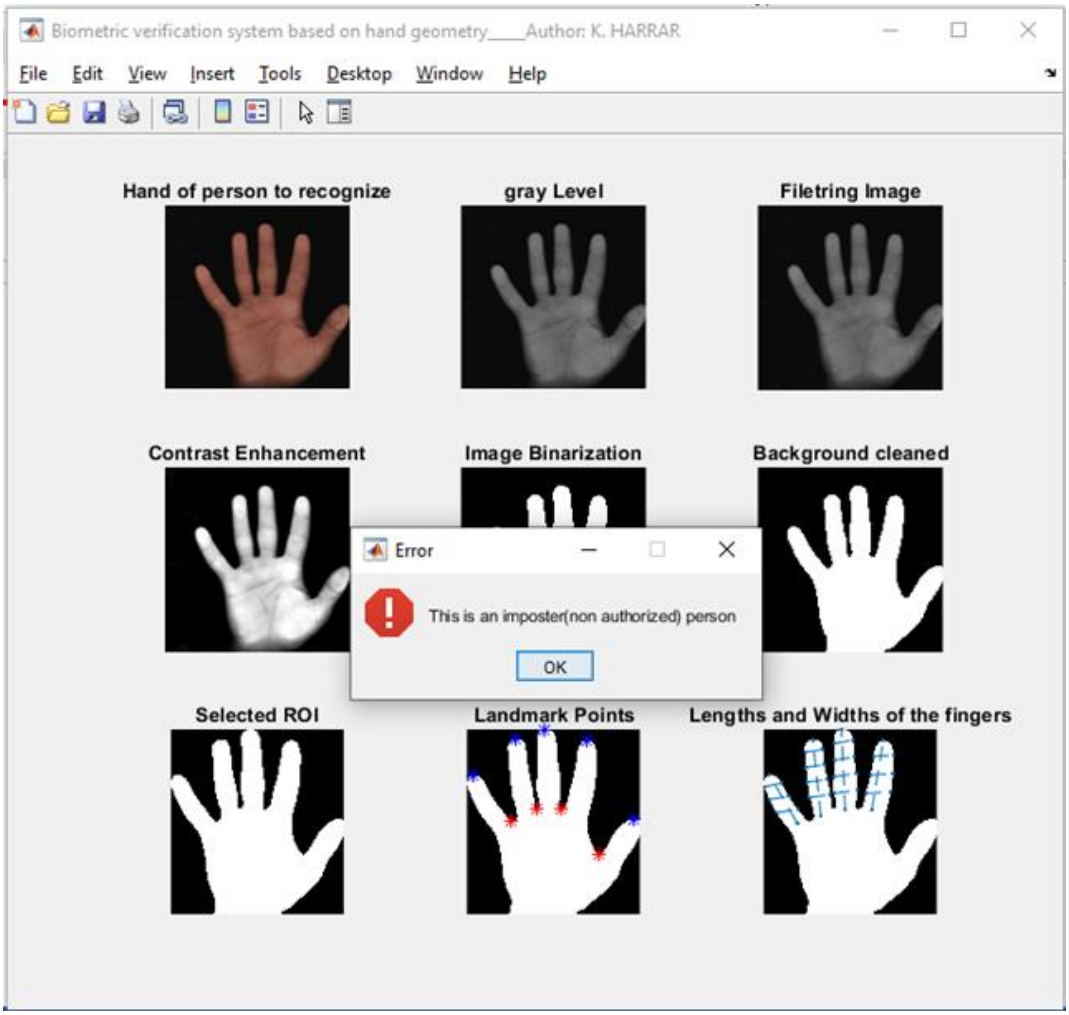

Fig.15. Example of an unauthorized person

4. CONCLUSION

The objective of this paper was to develop a verification system for recognizing persons based on hand geometry, using a combination of length and width of fingers. Several new features corresponding to various measurements at different places of fingers were introduced in this study. In this work, different sets of features have been evaluated and some experimental findings have been obtained. Despite the use of a small database, our system achieved an overall accuracy of 98.67% outperforming methods existing in the literature. From this study, we conclude that:

- The geometrical features of hand geometry systems affect the performance of those systems.
- Combining different geometrical features improved the performance of the recognition.

- The most discriminative geometrical features are related to the lengths of the four fingers in the case of taking into consideration a slightly different hand position during the process of acquisition.

For future work, the combination of the geometrical features with the hand texture features [31] can increase the performance of the system. Moreover, a large database could improve also the accuracy of the recognition.

5. REFERENCES

[1] Dargan S, Kumar M. A comprehensive survey on the biometric recognition systems based on physiological and behavioral modalities, Expert Syst. Appl., 2020, 143, doi: 10.1016/j.eswa.2019.113114

[2] Sharma S, Dubey S R, Singh S K, Saxena R, Singh R K. Identity verification using shape and geometry of human hands, Expert Sys. Appl., 2015, 42(2), 821-832, doi: 10.1016/j.eswa.2014.08.052

[3] Miroslav B, Grd P, Fotak T. Basic Principles and Trends in Hand Geometry and Hand Shape Biometrics, Article. Intech, 2012, pp. 77-99, doi: 10.5772/51912

[4] Klonowski M, Plata M, Syga P. User authorization based on hand geometry without special equipment, Pattern Recogn., 73, 2018, 189-201, doi: 10.1016/j.patcog.2017.08.017

[5] Barra S, Marsico M D, Nappi M, Narducci P, Riccio D. A hand-based biometric system in visible light for mobile environments, Inform. Sciences, 479, 2019, 472-485, doi: 10.1016/j.ins.2018.01.010

[6] Firas M, Salih Z. Authentication system depends on hand geometry using backpropagation neural network, JITBM & ARF. 2014, Université Polytechnique Iraq

[7] Burgues J, Fierrez J, Ramos D, Ortega-Garcia J. Comparison of Distance-Based Features for Hand Geometry Authentication. In: Fierrez J, Ortega-Garcia J, Esposito A, Drygajlo A, Faundez-Zanuy M (eds) Biometric ID Management and Multimodal Communication. BioID 2009. Lecture Notes in Computer Science, 5707. Springer, Berlin, Heidelberg, 2009

[8] Gross R, Li Y, Sweeney L, Jiang X, Xu W, Yurovsky D. Robust Hand Geometry Measurements for Person Identification using Active Appearance Models, IEEE, 2007, 1st

IEEE International Conference on Biometrics: Theory, Applications, and Systems, doi: 10.1109/BTAS.2007.4401936

[9] Goh M K O, Connie T, Teoh A B J. A contactless biometric system using multiple hand features, J. Vis. Commun. Image R., 23(7), 2012, 1068-1084, doi: 10.1016/j.jvcir.2012.07.004

[10] Shawkat S A, Lateef Al-Badri K S, Turki A I. The new hand geometry system and automatic identification, Period. Eng. Nat. Sci., 7(3), 2019, 996-1008, doi: 10.21533/pen.v7i3.632

[11] Appiah O, Asante A, Hayfron-Acquah J B. Improved approximated median filter algorithm for real-time computer vision applications, J. King Saud Univ., Comp. & Info. Sci., 2020, doi: 10.1016/j.jksuci.2020.04.005

[12] Singh R, Vatsa M, Noore A. Improving verification accuracy by synthesis of locally enhanced biometric images and deformable model, Signal Processing, 87(11), 2007, 2746-2764, doi: 10.1016/j.sigpro.2007.05.009

[13] Otsu N. A threshold selection method from gray-level histograms, IEEE Trans. Sys., Man., Cyber., 9, 1979, 62–66, doi: 10.1109/TSMC.1979.4310076

[14] Gonzalez R C, Woods R E, Eddins S L**.** Digital Image Processing Using MATLAB**,** New Jersey, Pearson Prentice Hall, 2004.

[15] Matos H, Oliveira H.P, Magalhães F. Hand-Geometry Based Recognition System. In: Campilho A., Kamel M. (eds) Image Analysis and Recognition, ICIAR 2012, Lecture Notes in Computer Science, vol 7325. Springer, Berlin, Heidelberg, doi: 10.1007/978-3-642-31298-4_5

[16] Ahuja M K, Singh A. (2015, Mar). A survey of hand geometry recognition. Ijarcsms. 3(3), 2015, 312-318

[17] Kolountzakis M N, Kutulakos K N, Fast computation of the Euclidian distance maps for binary images, Inform. Process. Lett., 43(4), 1992, 181-184, doi: 0.1016/0020-0190(92)90197-4

[18] Davydov V A. On Application of the Modulus Metric to Solving the Minimum Euclidean Distance Decoding Problem, Probl. Inf. Transm. 55, 2019, 145–151, doi:

10.1134/S0032946019020030

[19] Ohzeki K, Takatsuka M, Kajihara M. Hirakawa Y, Sato K. On the false rejection ratio of face recognition based on automatic detected feature points, Pattern Recognit. Image Anal. 26, 2016, 379–384, doi: 10.1134/S1054661816020073

[20] Ali S S, Baghel V S, Ganapathi I I, Prakash S. Robust biometric authentication system with a secure user template, Image Vision Comput., 104, 2020, doi: 10.1016/j.imavis.2020.104004

[21] Slooten K. Likelihood ratio distributions and the (ir) relevance of error rates, Forensic Sci. Int-Gen., 44, 2020, doi: 10.1016/j.fsigen.2019.102173

[22] Bapat A, Kanhangad V. Segmentation of hand from cluttered backgrounds for hand geometry biometrics, IEEE Region 10 Symposium, 2017, doi: 10.1109/TENCONSPRING.2017.8070016

[23] Bulatov Y, Jambawalikar S, Kumar P, Sethia S. Hand recognition using geometric classifiers, Lect. Notes Comput. Sc., 3072, 2004, 753-760, doi: 10.1007/978-3-540-25948-0_102

[24] Muthukumar A, Kavipriya A. A biometric system based on Gabor feature extraction with SVM classifier for Finger-Knuckle-Print, Pattern Recogn. Lett., 125, 2019, 150-156, doi: 10.1016/j.patrec.2019.04.007

[25] Hanley J A, McNeill B J. The meaning and use of the area under a Receiver Operating Characteristic (ROC) curve, Radiol., 143 (1), 1982, 29–36, doi: 10.1148/radiology.143.1.7063747

[26] Harrar K, Jennane R, Trabecular texture analysis using fractal metrics for bone fragility assessment, structure, 9(9), 2015, 683-688, doi: 10.5281/zenodo.1108242

[27] Sanchez-Reillo R, Sanchez-Avila C, Gonzalez-Marcos A. Biometric identification through hand geometry measurements, IEEE T. Pattern Anal., 22(10), 2000, 1168–1171, doi: 10.1109/34.879796

[28] Wong L, Shi P. Peg-free hand geometry recognition using hierarchical geometry and shape matching, in Proceedings of the IAPR Workshop on Machine Vision Applications, Nara, Japan, 2002, 281–284.

[29] Morales A, Ferrer M, Díaz F, Alonso J, Travieso C. Contact-free hand biometric system for real environments, in: Proceedings of the 16th European Signal Processing Conference (EUSIPCO), Laussane, Switzerland, 2008.

[30] Aundez-Zanuy M. Biometric verification of humans by means of hand geometry. In: 39th Annual 2005 International Carnahan Conference on Security Technology CCST, 2005, 61–67, doi: 10.1109/CCST.2005.1594816

[31] Harrar K, Khider M. Texture analysis using multifractal spectrum, International Journal of Modeling and Optimization 4 (4), 2014, 336-341, doi: 10.7763/IJMO.2014.V4.396

How to cite this article:
Harrar K. Biometric verification system based on hand geometry. J. Fundam. Appl. Sci., 2021, 13*(2), 816-844.*